Macromolecules

ARTICLE

pubs.acs.org/Macromolecules

Composite Fuel Cell Membranes from Dual-Nanofiber Electrospun Mats

Jason B. Ballengee and Peter N. Pintauro*

Department of Chemical and Biomolecular Engineering, Vanderbilt University, 2400 Highland Avenue, Nashville, Tennessee 37212, United States

Supporting Information

ABSTRACT: Nafion and poly(phenyl sulfone) are simultaneously electrospun into a dual-fiber mat. Follow-on processing of the mat produces two distinct membrane structures: (1) Nafion reinforced by a poly(phenyl sulfone) nanofiber network and (2) Nafion nanofibers embedded in inert/uncharged poly(phenyl sulfone) nanofiber network. For structure 1, the Nafion component of the fiber mat is allowed to soften and flow to fill the PPSU interfiber void space without damaging the PPSU fiber structure (by use of a mat compression step followed by thermal annealing). For structure 2, the PPSU material in the mat is allowed to soften and flow into the void space between Nafion nanofibers without damaging the Nafion fiber structure (by mat compression, exposure to chloroform solvent vapor, and then thermal annealing). Both membrane structures exhibit similar volumetric/gravimetric water swelling and proton conductivity, where the conductivity scales linearly with Nafion volume fraction and the swelling is less than expected based on the relative amounts of Nafion. The in-plane liquid water swelling of membranes with Nafion reinforced by a poly(phenyl sulfone) nanofiber network is always less than that of the inverse structure. On the other hand, the mechanical properties of membranes with Nafion nanofibers embedded in poly(phenyl sulfone) are superior to membranes with the opposite structure. Compared to other fuel cell membranes, the nanofiber composite membranes exhibit very low in-plane water swelling and better mechanical properties, which translates into improved membrane/MEA longevity in a hydrogen/air open circuit voltage humidity cycling durability test with no loss in power production as compared to a Nafion 212 membrane.

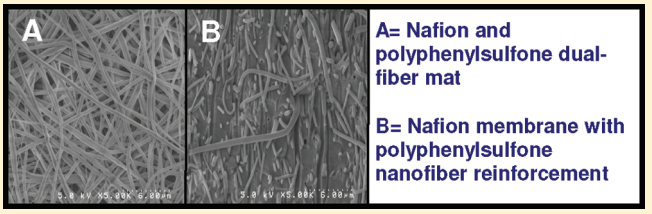

INTRODUCTION

Nafion has been widely studied as the membrane material in hydrogen/air fuel cells due to its high proton conductivity and inherent thermal/mechanical/chemical stability.[1] For long-term use with numerous on/off cycles, such as the case for automotive applications, researchers have found that Nafion undergoes undesirable dimensional swelling and shrinking which eventually leads to membrane degradation.[2,3] During hydrogen/air fuel cell operation at an elevated temperature (e.g., 80 °C), the proton-exchange membrane swells with water due to the presence of humid feed gases and the production of water at the cathode. After shutdown, the system cools, the supply of humid gases ceases, and the membrane dehydrates and shrinks. Tensile and compressive forces on the membrane are generated during membrane swelling/shrinking events due to physical constraints on the membrane (as part of the membrane electrode assembly, MEA) in a fuel cell fixture.[4] These forces cause unwanted membrane/electrode delamination, membrane creep, and pinhole formation.[5,6] Few membrane materials have been fabricated to address this problem, although there have been numerous studies where Nafion swelling has been investigated.[5,7−10]

Water swelling of a charged polymer can be controlled by the presence of physical cross-links. Such cross-links are generated by blending the ionomer with a hydrophobic/uncharged polymer. Solution cast blended films of Nafion and an uncharged polymer are problematic due to the incompatibility of Nafion with typical membrane casting solvents (i.e., Nafion forms a micellar dispersion and not a true polymer solution in typical membrane casting solvents such as dimethylformamide and dimethylacetamide) and with the uncharged polymer itself. With poorly dispersed blends there is little or no control of membrane swelling and no improvement in membrane mechanical properties.[11] Nonetheless, there have been a number of Nafion blending studies in the fuel cell literature involving the addition of poly(vinylidene fluoride) (PVDF).[12−15] One study found that PVDF and Nafion had poor miscibility below 60 wt % Nafion loading.[16] Water swelling was controlled (reduced from 37% for Nafion to ∼27% for a blend membrane with 80 wt % Nafion), but the proton conductivity was dramatically reduced (from 0.052 S/cm for neat Nafion to 0.012 S/cm for the Nafion/PVDF blend).

An alternative strategy to blended Nafion fuel cell membranes is an impregnated composite membrane construct. For fuel cell applications, the most well-known impregnated membrane material is the GORE-SELECT product line from W. L. Gore & Associates where Nafion is impregnated into an expanded

Received: July 21, 2011
Revised: August 22, 2011
Published: August 29, 2011

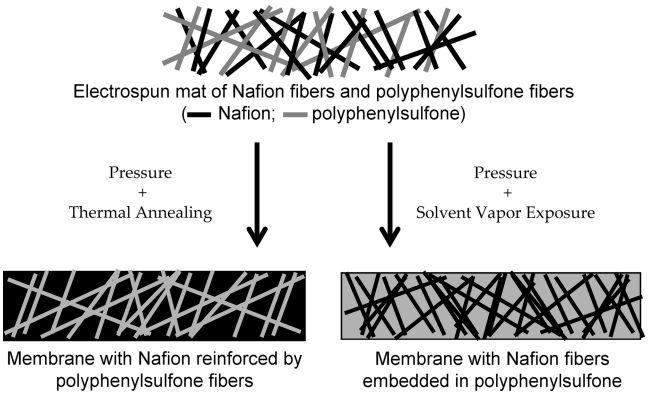

Figure 1. Creating two nanofiber-composite Nafion/poly(phenyl sulfone) membrane structures from the same dual fiber electrospun mat.

Teflon sheet. In one iteration of the GORE-SELECT membrane, the conductivity was half that of Nafion 112 (due to the presence of the inert PTFE support material), but dimensional stability was improved (linear in-plane shrinkage upon dehydration was reduced from 11% for Nafion to 3%).[17] The impregnation processing step is the primary drawback of this type of composite membrane material. Typically, multiple ionomer solution impregnations are required with intermittent solvent evaporation (membrane drying) steps. Complete filling of the inert matrix void volume is often challenging, and there could be undesirable membrane swelling issues if the solvent of the ionomer impregnation solution sorbs into the inert matrix polymer.

In the present paper, an alternative technique for fabricating composite ion-exchange membranes is presented. Two distinct membrane structures are described herein: (1) a Nafion film reinforced by a poly(phenyl sulfone) nanofiber network and (2) Nafion nanofibers embedded in inert/uncharged poly(phenyl sulfone) polymer nanofiber network. Whereas the latter structure is similar to that of GORE-SELECT films, the former is a new morphology for Nafion/hydrocarbon polymer blends. The two membrane types are fabricated from the same dual fiber mat that was formed by simultaneously electrospinning Nafion and poly(phenyl sulfone) (PPSU) from two separate spinnerets. Simple post-electrospinning processing steps were developed to create the two final membrane morphologies (see Figure 1). For structure 1, the Nafion component of the fiber mat is allowed to soften and flow to fill the PPSU interfiber void space without damaging the PPSU fiber structure (by use of a mat compression step followed by thermal annealing). For structure 2, the PPSU material in the mat is allowed to soften and flow into the void space between Nafion nanofibers without damaging the Nafion fiber structure (by mat compression, exposure to chloroform solvent vapor, and then thermal annealing). The method is inherently simpler and more robust than an impregnation scheme, and the final polymer morphology is not limited by dispersion/compatibility problems that often plague blended membrane systems. As will be shown below, the resulting nanofiber composite membranes have attractive properties for fuel cell applications.

The current work is an advancement over previously electrospun nanofiber-based fuel cell membranes in which ionomer fibers were electropun and impregnated with a hydrophobic polymer component.[18−22] Our new approach provides (i) ease of manufacture (no impregnation), (ii) versatility of morphology (two distinct structures are fabricated from the same dual fiber mat where the diameter and volume fraction of the nanofibers can be controlled), and (iii) a robust framework for future membrane design and fabrication (e.g., the method can be easily extended to other polymer composite combinations and the number of polymers incorporated into the composite membrane via electrospinning can be easily increased to three or more).

EXPERIMENTAL SECTION

Electrospinning. Separate Nafion and poly(ethylene oxide) (PEO) solutions were prepared by dissolving Nafion powder (prepared by evaporating the solvent from LIQUION 1115, Ion Power, Inc.) and PEO powder (Sigma-Aldrich, 400 kDa MW) into a 2:1 weight ratio *n*-propanol:water mixture. These two solutions were then combined to form a Nafion/PEO electrospinning solution where PEO constituted 1 wt % of the total polymer content.

Poly(phenyl sulfone) (Radel R 5500NT, 63 kDa MW, from Solvay Advanced Polymers, LLC) solutions were prepared by dissolving polymer powder in a 80:20 weight ratio of *n*-methyl-2-pyrrolidone: acetone. The poly(phenyl sulfone) (PPSU) solution and Nafion/PEO solution were each drawn into separate syringes and electrospun using 22 g needles (Hamilton Co.). PPSU fibers and Nafion/PEO fibers were simultaneously collected on a rotating aluminum drum that also oscillated laterally to ensure a random distribution and orientation of fibers with a uniform fiber density. The flow rates and concentrations of Nafion/PEO and PPSU were varied to produce fiber mats of varying compositions (i.e., different Nafion volume fractions). Nafion/PEO was electropsun at flow rates ranging from 0.10 to 0.60 mL/h and concentrations from 20 to 25 wt %. PPSU was electrospun at flow rates from 0.04 to 0.40 mL/h at a constant concentration of 25 wt %. For Nafion/PEO electrospinning, the spinneret-to-collector distance (SCD) was fixed at 5.5 cm, and the voltage was set between 3.75 and 4 kV. PPSU was electrospun at 7.5 kV with a SCD of 8.5 cm. All electrospinning experiments were performed at room temperature, where the relative humidity was 22−40%.

Nanofiber Mat Processing. Electrospun mats were processed in two different ways to give two distinct membrane morphologies.

Method 1 (for Membranes Where a Nafion Film Is Reinforced by a PPSU Nanofiber Network). The electrospun mat was compressed at 15 000 psi and 127 °C for ∼10 s. The sample was rotated 90° three times and successively compressed to ensure even compression. The mat was then annealed in vacuum at 150 °C for 2 h. The resulting membrane was boiled in 1 M sulfuric acid and deionized water for 1 h each to remove residual PEO and to protonate all ion-exchange sites. Membranes were fabricated with Nafion volume fractions ranging from 0.33 to 1.0. (For a membrane with a Nafion volume fraction of 1.0, a mat with no PPSU fibers was processed as described above.)

Method 2 (for Membranes Where Nafion Nanofibers Are Embedded in PPSU). Electrospun mats were compressed at 3500 psi and 23 °C. The sample was rotated 90° three times and successively compressed to ensure even compression. The mat was suspended above liquid chloroform at 23 °C (i.e., exposed to chloroform vapor) in a sealed jar for 8−16 min (depending on the Nafion volume fraction, e.g., 16 min for mats with 70 vol % Nafion; 8 min for mats with 30 vol % Nafion). The membranes were immediately dried at 70 °C for 1 h and then at 140 °C for 10 min, followed by thermal annealing of the Nafion (150 °C for 2 h under vacuum). The membranes were then boiled in 1 M sulfuric acid for 1 h and boiled in deionized water for 1 h. Membranes with Nafion nanofibers embedded in PPSU were fabricated with Nafion volume fractions ranging from 0.09 to 0.68. Membranes composed solely of PPSU (0.00 Nafion volume fraction) were fabricated from electrospun PPSU nanofiber mats by this same method.

Scanning Electron Microscopy. Electrospun mats and membranes were imaged with a Hitachi S-4200 scanning electron microscope. Samples were sputter-coated with a gold layer (~5 nm) to provide electrical conductivity. Freeze-fractured membrane cross sections were prepared by immersing samples in liquid nitrogen. Fiber diameters were calculated using the ImageJ software package.

Proton Conductivity. In-plane proton conductivity was measured by ac impedance. Water-equilibrated membrane samples were loaded into a BekkTech four-electrode cell and immersed in water. Conductivity was calculated using eq 1

$$\sigma = \frac{L}{Rw\delta} \tag{1}$$

where σ [S/cm] is proton conductivity, R [Ω] is the measured resistance between the electrodes, L [cm] is the distance between the electrodes, w [cm] is the width of the sample (usually 1 cm), and δ [cm] is the thickness of the sample (typically between 0.0030 and 0.0060 cm).

Ion-Exchange Capacity. Ion-exchange capacity (IEC) was determined by a standard acid exchange and base titration experiment. A membrane sample of known dry weight in the H^+ counterion form was soaked in 1 M NaCl for a minimum of 48 h to exchange protons with Na^+. The soak solution was then titrated to pH 7 with 0.01 N NaOH. IEC was calculated by eq 2

$$\text{IEC} = \frac{VN}{m_{\text{dry}}} \times 1000 \tag{2}$$

where IEC [mequiv/g] is ion-exchange capacity (on a dry polymer weight basis), V [L] is the volume of the NaOH titrating solution, N [mol/L] is the normality of the NaOH titrating solution, and m_{dry} [g] is the dry mass of the membrane. The Nafion volume fraction in a composite membrane was determined from the measured IEC, as per eq 3

$$\text{Nafion volume fraction} = \frac{\text{IEC}_{\text{composite}}}{\text{IEC}_{\text{Nafion}}} \frac{\rho_{\text{composite}}}{\rho_{\text{Nafion}}} \tag{3}$$

where $\text{IEC}_{\text{composite}}$ and $\rho_{\text{composite}}$ are the measured ion-exchange capacity and dry density of a nanofiber composite membrane and $\text{IEC}_{\text{Nafion}}$ and ρ_{Nafion} are the same quantities for a neat solution cast and annealed Nafion film.

Water Uptake and Swelling. Gravimetric, volumetric, and areal (in-plane) swelling (water uptake) were measured by boiling samples in 1 M sulfuric acid for 1 h and then boiling in 100 °C water for 1 h. Samples were removed from the water bath and quickly wiped dry, and then membrane mass, area, and volume were measured. Swelling was determined by eq 4

$$\text{water swelling } (\%) = \frac{x_{\text{wet}} - x_{\text{dry}}}{x_{\text{dry}}} \times 100 \tag{4}$$

where x is either the membrane's mass, geometric area, or volume, corresponding to mass swelling, in-plane/areal swelling, or volumetric swelling, respectively.

Mechanical Properties. Mechanical properties were measured with a TA Instruments Q800 dynamic mechanical analyzer (DMA). Stress−strain curves were obtained for dry membranes at 30 °C and ~20% RH (all membranes were predried at ambient conditions for a minimum of 3 days and in vacuum at 40 °C for 1 h before the measurements). The DMA was operated in tension using the controlled force mode, where the force was increased at 0.1000 N/min until the sample yielded.

Fuel Cell Polarization. Fuel cell polarization curves were obtained for a 5 cm^2 membrane electrode assembly (MEA) at a cell temperature of 80 °C, a feed gas humidity of 100%, and ambient pressure. For all experiments, the Pt electrode catalyst loading was 0.4 mg/cm^2, with 30 wt % Nafion binder. Catalyst inks were prepared from Pt/C catalyst (Alfa Aesar #42204) and Nafion solution (Sigma-Aldrich #527084). MEAs were fabricated using a standard decal method, where electrodes were painted onto Kapton films and then transferred to a membrane by hot-pressing for 10 min at 140 °C and 100 psi. Prior to a fuel cell test, the MEA was preconditioned overnight at room temperature by repeatedly cycling the cell for 5 min at a low current density (150 mA/cm^2) and then 5 min at a low voltage (0.2 V).[23] In a fuel cell experiment, feed gases were supplied at 100 mL/min (hydrogen) and 500 mL/min (air) for the anode and cathode, respectively. Polarization curves were obtained by measuring the current at specified voltages after 60 s of equilibration.

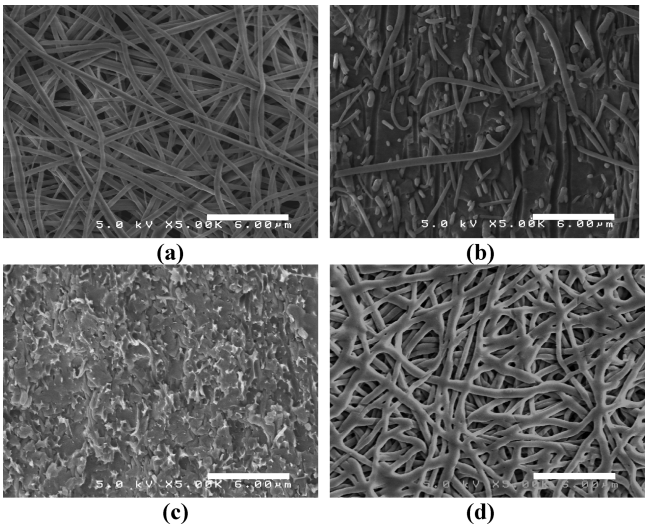

Figure 2. SEM micrographs of (a) an electrospun dual nanofiber mat surface (fibers are visually indistinguishable but are composed of either PPSU or Nafion), (b) freeze-fractured cross section of a Nafion film reinforced by a PPSU nanofiber network, (c) freeze-fractured cross section of a membrane with Nafion nanofibers embedded in PPSU, and (d) surface of the Nafion nanofiber structure membrane after removal of all PPSU (by soaking in liquid chloroform). Scale bars are 6 μm.

Fuel Cell Durability/Open-Circuit Voltage Experiment. Fuel cell durability was determined by an accelerated open-circuit voltage (OCV) test, where 100% and 0% hydrogen and air feed gases were successively and repeatedly passed through the fuel cell test fixture (2 min each), while continuously monitoring the OCV. A 25 cm^2 fuel cell was operated at 80 °C for the test. The catalyst layers were prepared via a decal method, as stated above. The hydrogen limiting current was periodically measured during an OCV experiment by linear sweep voltammetry (0.0−0.50 V, using a Gamry Series G300 potentiostat) after changing the feed gases (humidified hydrogen to the anode and nitrogen to the cathode at 200 mL/h).[2]

RESULTS AND DISCUSSION

Membrane Morphology. Nafion and poly(phenyl sulfone) (henceforth abbreviated as PPSU) solutions were simultaneously electrospun from separate syringes to produce a nanofiber mat. Electrospinning perfluorosulfonic acid (PFSA) polymer solutions (e.g., DuPont's Nafion in alcohol:water solvents) is difficult because PFSAs do not dissolve in normal organic solvents but rather form micellar dispersions. Without the requisite chain entanglements, such solutions can only be electrospun by addition of a neutral high molecular weight carrier polymer like poly(ethylene oxide) (PEO), poly(acrylic acid) (PAA), or poly(vinyl alcohol).[20,21,25] A high concentration of the carrier (as much as 25 wt %) was required in early studies to electrospin

Nafion fibers.[24−26] More recently, electrospinning conditions have been identified for electrospinning Nafion and other PFSA materials with a much lower concentration of the carrier material (e.g., ≤1 wt % PEO).[21,22,27] In the present study, Nafion and PEO (400 kDa MW) were mixed and electrospun in a 99:1 weight ratio (400 kDa MW) using a 2:1 *n*-propanol:water solvent. PEO was later removed from a fully processed membrane during the standard Nafion membrane pretreatment sequence of boiling in sulfuric acid and then boiling in water.

Figure 2a shows the fiber morphology of an electrospun mat containing Nafion/PEO and PPSU fibers where there is a uniform distribution of Nafion and PPSU nanofibers, with an average fiber diameter of 340 nm (the two types of fibers are indistinguishable in the SEM). In Figure 2a, 60% of the fibers are composed of Nafion/PEO fibers, as determined by ion-exchange capacity and membrane density measurements. In its present form, the dual fiber mat is highly porous and cannot be used as a fuel cell membrane, so further processing of the mat is required to create a dense and defect-free film. This processing can follow two different paths: (i) the Nafion/PEO fibers can fill the voids between PPSU fibers (resulting in a Nafion membrane reinforced by PPSU nanofibers), or (ii) the PPSU polymer can fill the void space between Nafion nanofibers, resulting in a membrane where proton conducting PFSA nanofibers are embedded in an inert/uncharged PPSU matrix.

The processing steps for converting a dual fiber electrospun mat into a Nafion membrane with reinforcing PPSU nanofibers are as follows: hot press at ∼15 000 psig and 127 °C and then anneal at 150 °C for 2 h (this time and temperature are the normal annealing conditions for Nafion). In a previous study, Choi et al.[20] observed that Nafion nanofibers in a low fiber volume fraction mat would fuse/weld at an elevated temperature, thus creating a three-dimensional PFSA nanofiber network. We have found in our work that Nafion nanofibers will soften, flow, and fully fill the void space between PPSU nanofibers when a high fiber volume fraction mat is subjected to a high-temperature annealing step. The softening and flow of Nafion/PEO nanofibers are attributed to partial plasticization of Nafion by trace amounts of adsorbed water and to morphological rearrangement of ionic and amorphous domains since compression and annealing occurs above Nafion's α-transition temperature (∼100 °C).[28,29] After annealing, the membrane is boiled in 1 M sulfuric acid and water (1 h each) to remove residual PEO from the membrane (the presence of PEO is known to suppress proton conductivity in a Nafion nanofiber membrane)[20] and to ensure that all sulfonic acid ion-exchange sites are in the proton counterion form. A freeze-fracture SEM cross section of a completely processed Nafion membrane reinforced by PPSU nanofibers is shown in Figure 2b. The PPSU fibers are clearly visible and uniformly distributed throughout the membrane thickness, and Nafion appears to completely fill the interfiber void volume.

A membrane with Nafion nanofibers embedded in PPSU (a morphology inverse to that in Figure 2b) was fabricated by compacting the mat at ∼3500 psig, exposing the mat to chloroform vapor at room temperature to induce softening and flow of PPSU into the void space between Nafion nanofibers, drying the mat to remove chloroform, and then annealing the Nafion at 150 °C for 2 h in vacuum. After the annealing step the membrane was pretreated in the normal fashion by boiling in sulfuric acid and water. A SEM freeze-fractured cross section of a membrane with Nafion nanofibers embedded in PPSU is shown in Figure 2c.

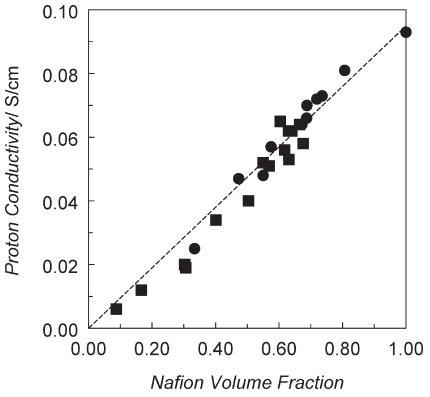

Figure 3. In-plane proton conductivity of nanofiber composite membranes as a function of Nafion volume fraction. Conductivity was measured in liquid water at room temperature. (■) Nafion nanofibers embedded in PPSU; (●) Nafion reinforced by PPSU nanofibers. Dashed line represents a simple volume fraction mixing rule (with zero ionic conductivity for PPSU) and Nafion 212 conductivity for a Nafion volume fraction of 1.0.

The Nafion fiber morphology cannot be seen in this image, so to confirm the membrane morphology a fully processed film was soaked in liquid chloroform for 2 h to dissolve/remove all of the PPSU. An SEM of the resulting membrane surface is shown in Figure 2d, where an interconnected (welded) network of Nafion nanofibers is clearly visible. Thus, it can be concluded that encapsulation of the Nafion nanofibers by PPSU prevents Nafion flow during the high-temperature annealing step, but it does allow for intersecting Nafion fibers to weld.

Membrane Properties. The in-plane proton conductivity of membrane samples for the two Nafion/PPSU composite structures in room temperature water is shown in Figure 3 as a function of Nafion volume fraction. There is no significant difference in conductivity between the two membrane morphologies, with proton conductivity being solely a function of the volume fraction of Nafion in the membrane (i.e., conductivity varies linearly with Nafion volume fraction, as shown by the straight line in Figure 3). Extrapolation of the linear data to a fiber volume fraction of 1.0 gives a proton conductivity identical to that of bulk Nafion (0.095 S/cm). The results in Figure 3 differ significantly from data in ref 30 where the authors report conductivities of a nonannealed electrospun Nafion fiber at 30 °C and 90% relative humidity that were unusually high (>1 S/cm) for small fibers (<300 nm diameter) and anomalously low (0.025 S/cm) for larger fibers (5 μm diameter).[30] In Figure 3, the membrane conductivities for the two different Nafion/PPSU morphologies obey the same Nafion volume fraction mixing rule (with zero conductivity for PPSU), as has been reported for other nanofiber composite fuel cell membranes.[18−22] Also, there is no percolation threshold for conductivity at low Nafion volume fractions; composite films with as little as 9 vol % Nafion fit the linear straight line conductivity correlation. This is well below the 16−30 vol % ionomer percolation minimum for composite membranes fabricated by traditional blending methods.[31,32] Furthermore, the proton conductivities of the nanofiber composite films are much higher than those reported for Nafion/PVDF solution-cast blends. For example, a solution-cast Nafion/PVDF film with 80 wt % Nafion was found to have a conductivity of 0.012 S/cm in water at 25 °C (23% the measured conductivity for a neat Nafion film), whereas a nanofiber composite of similar

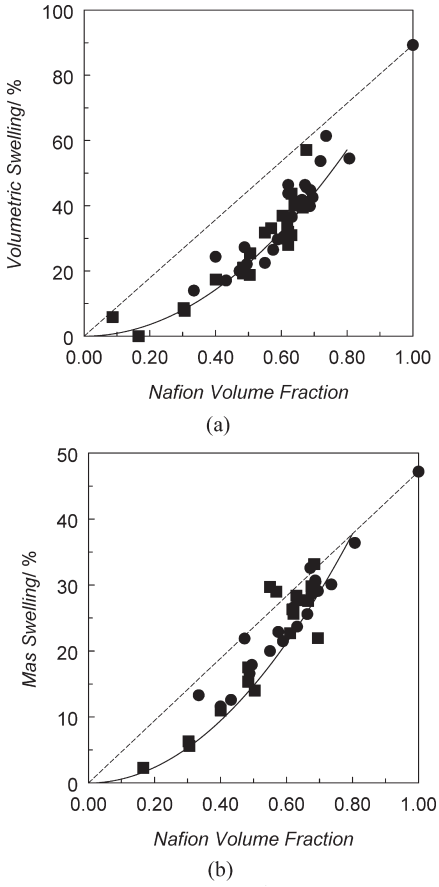

Figure 4. Water swelling of nanofiber composite membranes as a function of Nafion volume fraction at 100 °C. (a) Volumetric swelling. (b) Mass swelling. (■) Nafion nanofibers embedded in PPSU; (●) Nafion reinforced by PPSU nanofibers.

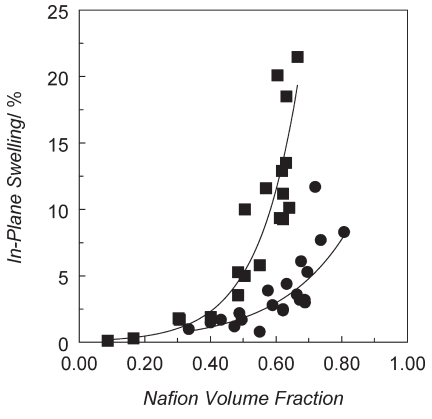

Figure 5. In-plane water swelling of nanofiber composite membranes as a function of Nafion volume fraction. Swelling was measured in 100 °C water. (■) Nafion nanofibers embedded in PPSU; (●) Nafion reinforced by PPSU fibers.

Nafion content has a conductivity of 0.070 S/cm, or 70% that of neat Nafion. (Note that nanofiber composite membranes that are ∼80 wt % Nafion are ∼70 vol % Nafion due to differences in Nafion's and PPSU's density.)

Volumetric and gravimetric water swelling of the two Nafion/PPSU composite membrane structures is shown in Figure 4 as a function of Nafion volume fraction. As was the case for proton conductivity, there is no obvious difference in swelling for the two different membrane structures (Nafion nanofibers embedded in PPSU and Nafion reinforced by a PPSU nanofiber network). However, the swelling is lower than would be predicted by a simple Nafion volume fraction mixing rule below 70 vol % Nafion (but not so low as to adversely affect proton conductivity) because the presence of PPSU causes the Nafion component to swell less in the composite films (this has been observed in other Nafion blended membranes).[32] For example, a membrane with 50 vol % Nafion has a λ (moles of water per mole of sulfonic acid sites in Nafion) of 19 as compared to 21.5 for commercial Nafion 212. The low water content of the composite membranes in Figure 4 is an important finding in terms of future applications of the membrane fabrication method with very high ion-exchange capacity (IEC) ionomer polymers that swell excessively in water.

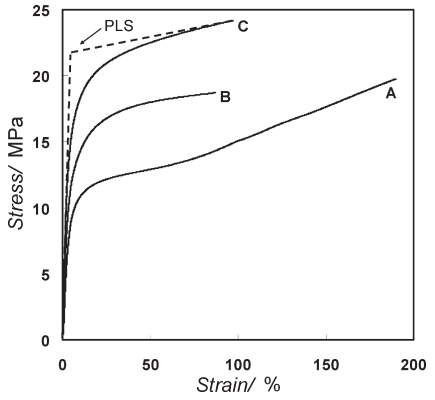

Figure 6. Stress−strain curves for Nafion 212 and nanofiber composite membranes. Stress−strain curves were measured at 30 °C and ∼20% RH: (a) Nafion 212, (b) Nafion reinforced by PPSU nanofibers (61 vol % Nafion), and (c) Nafion nanofibers embedded in PPSU (61 vol % Nafion).

In-plane (areal) water swelling of the two nanofiber composite membranes is shown in Figure 5 for films of different Nafion volume fraction. Unlike conductivity and volumetric/mass swelling, the in-plane swelling for the two membrane morphologies differ substantially, with Nafion films reinforced by PPSU nanofibers swelling less for a wide range of Nafion volume fractions. The swelling difference is attributed to differences in PPSU connectivity for the two membrane structures. A membrane with Nafion fibers embedded in PPSU has strong interconnectivity in three dimensions, with more isotropic water swelling. When PPSU is in the fiber form, there is minimal PPSU connectivity in the membrane thickness direction (the PPSU nanofibers were never welded to create a 3-D interconnecting network), with stronger connectivity for the in-plane direction (due to the presence of closed-form cells created by the PPSU fiber network). Thus, there is more membrane swelling in the thickness direction for membranes with reinforcing PPSU nanofibers, as compared to the inverse structure. For example, a membrane with 60 vol % Nafion had a thickness swelling of 29% for the Nafion film reinforced by PPSU nanofibers, but only 18% for the membrane with Nafion fibers embedded in PPSU. It should be noted that the in-plane swelling of both composite membrane morphologies was lower than that of neat Nafion (37% in-plane swelling for Nafion 212) and lower than that of a hypothetical PPSU/Nafion composite film based on a simple

Table 1. Young's Modulus and Proportional Limit Stress (PLS) for Nanofiber Composite Membranes of Different Nafion Volume Fractions

	Nafion nanofibers embedded in PPSU		Nafion reinforced by PPSU nanofibers	
Nanofiber composite	Young's modulus (MPa)	PLS (MPa)	Young's modulus (MPa)	PLS (MPa)
61 vol % Nafion	566	21.1	444	15.9
48 vol % Nafion	733	24.6	601	22.3
39 vol % Nafion	852	29.2	624	23.4
Neat membrane	Young's modulus (MPa)		PLS (MPa)	
Nafion 212	294		11.9	
poly(phenyl sulfone) film	1057		64.3	

Nafion volume fraction mixing rule. The swelling properties of the Nafion/PPSU nanofiber membranes compare favorably with other composite membranes found in the literature. A Nafion film reinforced by PPSU nanofibers had ~0.080 S/cm conductivity (in room temperature water) and an in-plane swelling of 8%, compared to 15% for a film of similar conductivity, as report by Lee and co-workers for a Nafion nanofiber mat impregnated with Norland Optical Adhesive 63.[22] Similarly, a GORE-SELECT membrane with a conductivity similar to that of Nafion 212 has a reported in-plane water swelling of ~31% in 100 °C water.[33] Under similar experimental conditions, the Nafion film reinforced by PPSU fibers exhibited 73% lower in-plane swelling with a small (20%) loss in proton conductivity relative to the GORE-SELECT film. (The loss in proton conductivity can be offset by simply making the membrane 20% thinner; changing membrane thickness will not alter in-plane swelling.)

PPSU has excellent mechanical properties, and its presence improved the overall mechanical properties of the nanofiber composite membranes, as compared to commercial Nafion films. Typical stress−strain curves for the two nanofiber composite membrane structures and for Nafion 212 are shown in Figure 6. Mechanical properties (Young's modulus and the proportional limit stress, abbreviated as PLS) are summarized in Table 1. PLS is a measure of yield strength which is useful for characterizing materials such as Nafion that do not undergo a clear transition from elastic to plastic deformation; PLS is determined by extrapolating lines tangent to the low- and high-strain regions of a stress−strain curve,[34] as shown in Figure 6. As can be seen, the nanofiber composite membranes have a higher modulus and proportional limit stress than Nafion 212, and the mechanical properties improve as the volume fraction of PPSU in the composite membrane increases. For all Nafion volume fractions tested, the membranes with Nafion nanofibers embedded in PPSU exhibited superior mechanical properties as compared to the inverse morphology. This is attributed to the greater connectivity of PPSU when it is the matrix material, surrounding Nafion nanofibers in a membrane, as opposed to having PPSU in the fiber form as a reinforcing nonwoven network.

Fuel Cell Performance. The low in-plane swelling of a Nafion film reinforced by PPSU nanofibers should translate into improved membrane electrode assembly (MEA) durability in a hydrogen/air fuel cell. To test this hypothesis, fuel cell data were collected for such a film containing 65 vol % Nafion. At this Nafion volume fraction, the membrane had a conductivity of

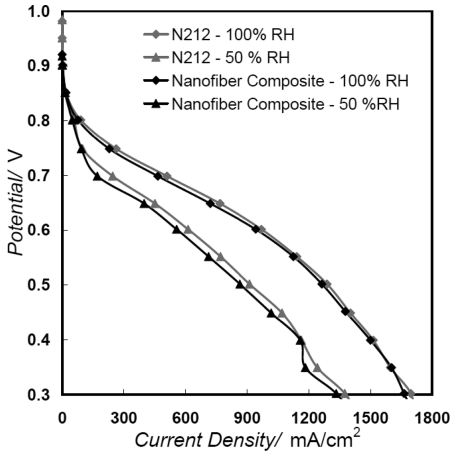

(a)

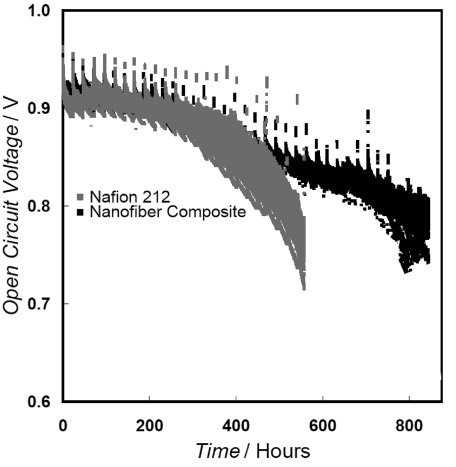

(b)

Figure 7. Fuel cell polarization (a) and accelerated durability tests (b). The nanofiber composite membrane (with Nafion reinforced by PPSU nanofibers) was ~65 vol % Nafion and 31 μm thick for all fuel cell testing.

0.066 S/cm in water (at 25 °C) and an in-plane swelling of 6% in 100 °C water. The composite film was fabricated into a MEA by attachment of Pt/C catalytic powder electrodes using a standard decal technique (see Experimental Section). Voltage vs current density fuel cell performance curves are shown in Figure 7a for a 30 μm PPSU/Nafion membrane and a commercial Nafion 212 film (51 μm dry thickness) at 80 °C for two different feed gas humidification levels. The area-specific resistance of the Nafion 212 and nanofiber composite membranes is approximately the same (the composite membrane has 65% of the conductivity and 60% of the thickness), and the fuel cell power output (voltage multiplied by current density) is essentially identical for the two MEAs. The high open-circuit voltage and low gas crossover (<2 mA/cm^2) for the composite membrane MEA indicates a membrane free of pinholes and defects.

Membrane durability was evaluated by an open-circuit voltage (OCV) humidity cycling experiment at 80 °C with repeated cycling of 2 min 100% relative humidity (RH) hydrogen gas and air and then 2 min 0% RH hydrogen and air. This OCV experiment was used to evaluate the membrane for both mechanical durability (the membrane undergoes stresses from swelling and

shrinking when the gases cycle between wet and dry) and chemical durability (the diffusion of hydrogen and oxygen into the membrane can result in the formation of harmful peroxides which can degrade Nafion for both the neat membrane and nanofiber composite).[35] In the present study, only OCV and hydrogen gas crossover were monitored during humidity cycling; there was no attempt to quantify any membrane chemical degradation with time by measuring, for example, fluoride release rates. The change in OCV (during the wet cycle) vs time is shown in Figure 7b. Failure criteria for this test is defined as a drop in OCV (for a fully humidified MEA) below 0.8 V. As can be seen, the nanofiber composite membrane failed after 842 h vs 546 h for Nafion 212 (a 54% improvement in membrane durability). Additionally, the hydrogen limiting current (measured in situ at 100% RH) dramatically increased at membrane failure (increasing from <2 mA/cm^2 at the beginning of the test to over 13 mA/cm^2 at failure; see Supporting Information). The durability of the inverse nanofiber composite membrane structure (Nafion nanofibers embedded in PPSU) has not yet been evaluated in a fuel cell; such data will be the subject of a future publication.

CONCLUSIONS

A new approach to the design and fabrication of composite ion-exchange membranes has been presented. Nanofiber mats of two dissimilar polymers (Nafion perfluorosulfonic acid polymer and poly(phenyl sulfone)) were simultaneously and separately electrospun into the same mat, and then the resulting dual fiber web was processed into two different defect-free dense film morphologies: (1) a Nafion film reinforced by poly(phenyl sulfone) nanofibers and (2) an interconnecting nanofiber mat of Nafion embedded in poly(phenyl sulfone). The procedures for converting a dual-fiber mat into either of the two membrane morphologies is simple and straightforward. Both membrane structures exhibited similar volumetric/gravimetric water swelling and proton conductivity, where the conductivity scaled linearly with Nafion volume fraction and the swelling was less than expected based on the relative amounts of Nafion and poly(phenyl sulfone). Compared to other fuel cell membranes, the nanofiber composite membranes exhibited very low in-plane water swelling and better mechanical properties, which translated into improved membrane/MEA longevity in a hydrogen/air open-circuit voltage humidity cycling durability test with no loss in power production as compared to a Nafion 212 membrane. The in-plane liquid water swelling of membranes with Nafion reinforced by a poly(phenyl sulfone) nanofiber network was always less than that of the inverse structure. On the other hand, the mechanical properties of membranes with Nafion nanofibers embedded in poly(phenyl sulfone) were superior to membranes with the opposite structure.

The impregnation-free dual-fiber electrospinning approach to composite membrane design can be expanded to produce composite films with any two polymers that are (i) electrospinnable and (ii) have sufficient differences in solubility and/or thermal properties so as to allow for one component to soften, flow, and fill the interfiber void volume of the other. Additionally, one can fabricate a composite membrane for non-fuel-cell applications, e.g., as separators in electrochemical reactors, for sensors, and in industrial electrodialysis separations. Also, it is entirely possible to fabricate nanofiber composite membranes with three or more different fiber compositions, e.g., one charged polymer for normal fuel cell operating temperatures, a second nanofiber for low (subzero) fuel-cell operation, and a third polymer fiber for membrane reinforcement.

ASSOCIATED CONTENT

Supporting Information. Figures showing a schematic of a dual-fiber electrospinning experiment and limiting current measurements from accelerated lifetime testing. This material is available free of charge via the Internet at http://pubs.acs.org.

AUTHOR INFORMATION

Corresponding Author
*E-mail: peter.pintauro@vanderbilt.edu.

ACKNOWLEDGMENT

The authors thank the US DOE Hydrogen Program (Award DE-FG36-06GO16030) for their financial support of this work.

REFERENCES

(1) Grot, W. G.; Rajendran, G. US Patent 5919583, 1999.
(2) Tang, H.; Peikang, S.; Jiang, S. P.; Wang, F.; Pan, M. *J. Power Sources* **2007**, *170* (1), 85–92.
(3) Huang, X. Y.; Solasi, R.; Zou, Y.; Feshler, M.; Reifsnider, K.; Condit, D.; Burlatsky, S.; Madden, T. *J. Polym. Sci., Part B: Polym. Phys.* **2006**, *44* (16), 2346–2357.
(4) Wu, J.; Yuan, X. Z.; Martin, J. J.; Wang, H.; Zhang, J.; Shen, J.; Wu, S.; Merida, W. *J. Power Sources* **2008**, *184* (1), 104–119.
(5) Kusoglu, A.; Karlsson, A. M.; Santare, M. H.; Cleghorn, S.; Johnson, W. B. *J. Power Sources* **2006**, *161* (2), 987–996.
(6) Patil, Y. P.; Jarrett, W. L.; Mauritz, K. A. *J. Membr. Sci.* **2011**in press.
(7) Kundu, S.; Simon, L. C.; Fowler, M.; Grot, S. *Polymer* **2005**, *46* (25), 11707–11715.
(8) Kusoglu, A.; Karlsson, A. M.; Santare, M. H.; Cleghorn, S.; Johnson, W. B. *J. Power Sources* **2007**, *170* (2), 345–358.
(9) Bauer, F.; Denneler, S.; Willert-Porada, M. *J. Polym. Sci., Part B: Polym. Phys.* **2005**, *43* (7), 786–795.
(10) Sethuraman, V. A.; Weidner, J. W.; Haug, A. T.; Protsailo, L. V. *J. Electrochem. Soc.* **2008**, *155*, B119–B124.
(11) Kerres, J. A. *Fuel Cells* **2005**, *5* (2), 230–247.
(12) Taylor, E. P.; Landis, F. A.; Page, K. A.; Moore, R. B. *Polymer* **2006**, *47* (21), 7425–7435.
(13) Landis, F. A.; Moore, R. B. *Macromolecules* **2000**, *33* (16), 6031–6041.
(14) Kyu, T.; Yang, J. C. *Macromolecules* **1990**, *23* (1), 176–182.
(15) Yang, J. C.; Kyu, T. *Macromolecules* **1990**, *23* (1), 182–186.
(16) Song, M.-K.; Kim, Y.-T.; Fenton, J. M.; Kunz, H. R.; Rhee, H.-W. *J. Power Sources* **2003**, *117* (1−2), 14–21.
(17) Kolde, J. A.; Bahar, B.; Wilson, M. S.; Zawodzinski, T. A.; Gottesfeld, S. *Electrochem. Soc. Proc.* **1995**, *95−23*, 193–201.
(18) Choi, J.; Lee, K. M.; Wycisk, R.; Pintauro, P. N.; Mather, P. T. *Macromolecules* **2008**, *41* (13), 4569–4572.
(19) Choi, J.; Lee, K. M.; Wycisk, R.; Pintauro, P. N.; Mather, P. T. *J. Electrochem. Soc.* **2010**, *157* (6), B914–B919.
(20) Choi, J.; Lee, K. M.; Wycisk, R.; Pintauro, P. N.; Mather, P. T. *J. Mater. Chem.* **2010**, *20* (30), 6282–6290.
(21) Choi, J.; Wycisk, R.; Zhang, W. J.; Pintauro, P. N.; Lee, K. M.; Mather, P. T. *ChemSusChem* **2010**, 3 (11), 1245–1248.
(22) Lee, K. M.; Choi, J.; Wycisk, R.; Pintauro, P. N.; Mather, P. *J. Electrochem. Soc.* **2009**, *25*, 1451–1458.
(23) Muldoon, J.; Lin, J.; Wycisk, R.; Takeuchi, N.; Hamaguchi, H.; Saito, T.; Hase, K.; Stewart, F. F.; Pintauro, P. N. *Fuel Cells* **2009**, *9* (5), 518–521.

(24) Chen, H.; Snyder, J. D.; Elabd, Y. A. *Macromolecules* **2008**, *41* (1), 128–135.
(25) Laforgue, A.; Robitaille, L.; Mokrini, A.; Ajji, A. *Macromol. Mater. Eng.* **2007**, *292* (12), 1229–1236.
(26) Zhou, C. S.; Liu, Z.; Dai, J. Y.; Xiao, D. *Analyst* **2010**, *135* (5), 1004–1009.
(27) Ballengee, J. B.; Pintauro, P. N. *J. Electrochem. Soc.* **2011**, *158* (5), B568–B572.
(28) Osborn, S. J.; Hassan, M. K.; Divoux, G. M.; Rhoades, D. W.; Mauritz, K. A.; Moore, R. B. *Macromolecules* **2007**, *40* (10), 3886–3890.
(29) Page, K. A.; Landis, F. A.; Phillips, A. K.; Moore, R. B. *Macromolecules* **2006**, *39* (11), 3939–3946.
(30) Dong, B.; Gwee, L.; Salas-de la Cruz, D.; Winey, K. I.; Elabd, Y. A. *Nano Lett.* **2010**, *10* (9), 3785–3790.
(31) McLachlan, D. S.; Blaszkiewicz, M.; Newnham, R. *J. Am. Ceram. Soc.* **1990**, *73* (8), 2187–2203.
(32) Lin, J.; Lee, J. K.; Kellner, M.; Wycisk, R.; Pintauro, P. N. *J. Electrochem. Soc.* **2006**, *153* (7), A1325–A1331.
(33) Cleghorn, S.; Kolde, J.; Liu, W. In *Handbook of Fuel Cells - Fundamentrals, Technology and Applications*; Vielstich, W., Lamm, A., Gasteiger, H. A., Eds.; John Wiley & Sons, Ltd.: Chichester, 2003; Vol. 3, pp 566−575.
(34) Tang, Y. L.; Karlsson, A. M.; Santare, M. H.; Gilbert, M.; Cleghorn, S.; Johnson, W. B. *Mater. Sci. Eng., A* **2006**, *425* (1−2), 297–304.
(35) de Bruijn, F. A.; Dam, V. A. T.; Janssen, G. J. M. *Fuel Cells* **2008**, *8* (1), 3–22.